PAPER

Role of chelate complexes in densification of CuInSe$_2$ (CIS) thin film prepared from amorphous Cu–In–Se nanoparticle precursors

Kyunhwan Kim, Young-Joo Eo, Ara Cho, Jihye Gwak, Jae Ho Yun, Keeshik Shin, Seoung Kyu Ahn, Sang Hyun Park, Kyunghoon Yoon and SeJin Ahn*

CuInSe$_2$ (CIS) absorber layers for thin film solar cells were fabricated *via* a non-vacuum route using amorphous Cu–In–Se nanoparticle precursors prepared by a low temperature colloidal process within one minute of reaction without any external heating. In particular, we intentionally added a chelating agent to the nanoparticle colloid in order to increase the density of the final films by enhancing the viscous flow of precursor materials during high temperature selenization. This is based on the decreased reactivity of precursor particles due to the formation of chelate complexes at particle surfaces. While the CIS films formed from the amorphous Cu–In–Se particles without surface modification were found to have large voids, those formed from surface modified particles showed flat and dense morphologies. In accordance with the improvements in the film morphology and density, efficiencies of the devices were also significantly increased from 0% (complete short circuit in the case without surface modification) to 4.41% (with surface modification).

Introduction

In spite of the high conversion efficiency (>20%) of state-of-the-art I–III–VI compound thin film solar cells, which was achieved by CuInGaSe$_2$ absorber films,[1,2] the high production cost and the difficulties in scaling up of the vacuum-based processes for forming the absorber layers such as a multi-stage co-evaporation and a sputtering/selenization are considered to be the main obstacles for the widespread use of the CIGS solar cells.[3,4]

In this regard, fabrication of CIS type thin films using nanoparticle based inks is considered to be one of the most promising low cost processes. Advantages of the CIS nanoparticle based approach include a dispersibility of the particles in organic solvents for non-vacuum coating[5] and a relatively easy compositional control of the final thin films[6] based on the fact that composition of the precursor nanoparticles can be directly transferred to that of as-coated[3,4,7] and selenized films[8] without noticeable change in the atomic ratios of elements. The latter further leads to an excellent composition control of the coated films even when there are some inhomogeneities in deposition processes.[3]

Among the previously reported preparation methods of CIS-type nanomaterials including solvothermal routes[9–12] and hot injection methods using a Schlenk line,[13–16] the low temperature colloidal process was reported to be a potential low cost alternative in that it can produce amorphous Cu–In–Se nanoparticles within a very short reaction time (~1 min) without any external heating.[7,17,18] In addition, due to the existence of a Cu–Se binary in the amorphous nanoparticle colloids, a facile growth of the particles up to a few μm scale by selenization was demonstrated, which was claimed as another merit of this method.[18] As a proof of concept, a completed solar cell prepared from the amorphous Cu–In–Se nanoparticles with a conversion efficiency of about 2% was also demonstrated.[18] However, it should be pointed out that the CIS films fabricated with the amorphous Cu–In–Se nanoparticles have suffered from high porosity due to the non-uniform growth of the particles during selenization,[18] meaning that facile growth of the amorphous particles was realized but film densification was not achieved. In this regard, to fully utilize the simple and fast nature of the low temperature colloidal process as an economical preparation method of nanoparticle precursors for CIS films, one needs an alternative strategy to increase the density of the final films.

On the other hand, it has been reported that, in solution based processes for forming inorganic thin films, addition of different chelating agents to the precursor solution significantly affected the densification behaviour of the films during high temperature sintering.[19] Schwartz found that zirconia films prepared from acetate (acetic acid)- or acetylacetone (acac)-modified zirconium *n*-butoxide, sintered at 700 °C, had different densities, in which films prepared from the acac precursor solution densified to a greater extent.[19] The implication of this report is that the lower reactivity of the precursors modified by larger chelating agents allows for film densification by structural relaxation and viscous flow, rather than solid-state sintering, finally leading to a formation of denser films.[19]

Solar Energy Department, Korea Institute of Energy Research, 71-2 JangDong, YuseongGu, DaeJeon, 305-343, Korea. E-mail: swisstel@kier. re.kr; Fax: +82-42-860-3739; Tel: + 82-42-860-3541

8444 | *J. Mater. Chem.*, 2012, **22**, 8444–8448

This journal is © The Royal Society of Chemistry 2012

In the same manner, in this work, we investigated the effects of surface modification of amorphous Cu–In–Se nanoparticles, by adding a chelating agent to the coating slurry, on the densification behaviour of the selenized films. The main intention of using the chelating agent here is to form chelate complexes at the surface of particles which are expected to delay the onset of crystallization during selenization and hence to enhance the viscous flow of particles and the densification of the films. Monoethanolamine (MEA) is chosen as a representative chelating agent based on previous papers reporting that MEA has been successfully used to chelate Cu[20,21] and In[20] ions. In addition, the monodentate characteristic of MEA may allow us to minimize the amount of residual carbon in the final films due to its easy dissociation property.

Here, we report that the chelating agent assisted route resulted in CIS thin films, prepared from the amorphous Cu–In–Se nanoparticles, with significantly improved morphologies and high density. Thin film solar cells fabricated with those absorber layers demonstrated a conversion efficiency of up to 4.41%, while the devices fabricated from the particles without chelation showed a complete short circuiting behavior.

Experimental section

Materials

CuI (99.999%), InI$_3$ (99.999%) and Na$_2$Se (99.8%) were purchased from Alfa Aesar, pyridine (99.9%) and MEA (99.0%) from Sigma Aldrich, methanol (99.6%) from Junsei, and elemental Se (99.999%, 3 mm shot) from Cerac.

Synthesis of precursor nanoparticles

Amorphous Cu–In–Se nanoparticles were synthesized according to the low temperature colloidal process reported by Schulz[7] and Ahn,[17] where a mixture of CuI (0.343 g) and InI$_3$ (0.991 g) in pyridine (30 ml) was reacted with Na$_2$Se (0.5 g) in methanol (20 ml) at 0 °C in an ice bath for 1 minute under nitrogen gas atmosphere with mechanical stirring. During the chemical treatment, the NaI by-product was removed from the product mixture with the remaining Cu–In–Se nanoparticles forming a stable methanol colloid.

Thin film coating

A coating slurry was prepared by adding a small amount of MEA to the Cu–In–Se nanoparticle/methanol colloid. The final mixtures were stirred with a magnetic bar vigorously for 30 minutes. Precursor films were formed by doctor blading (Multi coater, DCN Co. Ltd., Korea) the slurrys on a 1 μm thick Mo-coated soda-lime glass. The samples were then dried at 80 °C for 5 minutes and at 300 °C for 10 minutes in air on a hot plate to remove the solvent and the organic additive, respectively.

Selenization

Selenization was performed in a vacuum evaporator equipped with a Knudsen-type effusion cell. Initially the chamber was evacuated to a base pressure of 5×10^{-6} Torr with a turbo molecular pump and then elemental Se was evaporated from the effusion cell. All the samples were selenized at 530 °C for 30 minutes with Se flux corresponding to 10 Å s^{-1}.

Solar cell fabrication

Solar cells were fabricated according to the conventional Mo/CIS/CdS/i-ZnO/n-ZnO/Al structure. A 60 nm thick CdS buffer layer was deposited on a CIS film by chemical bath deposition (CBD) and i-ZnO(50 nm)/Al-doped n-ZnO(500 nm) was deposited by radio-frequency (rf) magnetron sputtering on the CdS layer. An Al grid of 500 nm thickness was deposited as a current collector using thermal evaporation. The active area of the completed cell was 0.44 cm².

Characterization

Morphology, composition and crystal structure of the nanoparticles, the precursor films and the selenized films were investigated by high-resolution scanning electron microscopy (HRSEM, XL30SFEG Phillips Co., Holland at 10 kV), Energy Dispersive Spectroscopy (EDS, EDAX Genesis apex, acceleration voltage: 30 kV, collection time: 100 s with standard-less method) and X-ray diffraction (XRD, Rigaku Japan, D/MAX-2500) using a CuKα line, respectively. Raman spectra of the selenized films were taken in the quasi-backscattering geometry by using the 514.5 nm line of an Ar ion laser as the excitation source. The scattered light was filtered with a holographic edge filter and dispersed by a Spex 0.55 m spectrometer and detected with a liquid-nitrogen-cooled back-illuminated charge-coupled-device (CCD) detector array. Depth compositional profile of the selenized film was obtained by Auger electron spectroscopy (AES, Perkin Elmer, SAM 4300).

Device performances including the conversion efficiency and the EQE (External Quantum Efficiency) were characterized using a class AAA solar simulator (WXS-155S-L2, WACOM, Japan) and an IPCE (Incident Photon Conversion Efficiency) measurement unit (PV Measurements, Inc., USA), respectively.

Results and discussion

Precursor nanoparticles

A typical SEM micrograph of the amorphous Cu–In–Se nanoparticles prepared by the low temperature colloidal route is shown in Fig. 1. Spherical nanoparticles of about 40 nm in
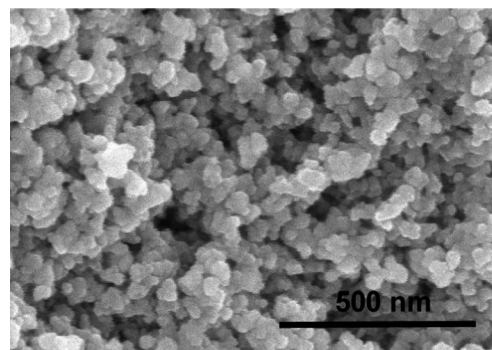

Fig. 1 SEM image of the amorphous Cu–In–Se nanoparticles.
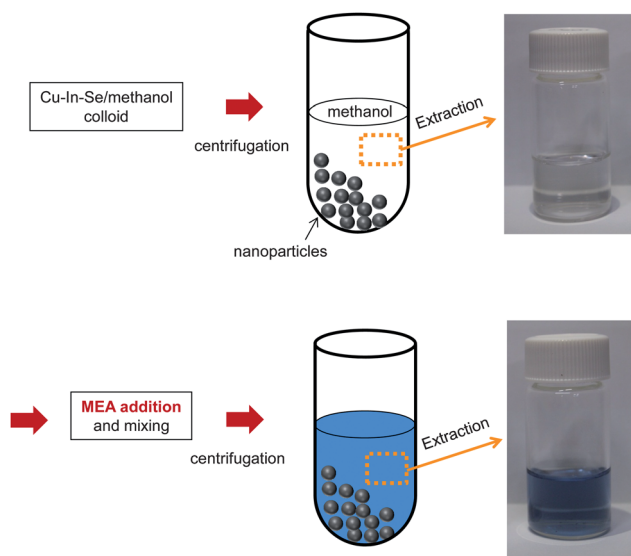
diameter with quite uniform size distribution were demonstrated. The structure and phase constitutions of the particles were reported in our previous paper,[18] in which it was revealed that the particles are in amorphous state and particularly that they are mixtures of amorphous Cu–Se and In–Se binary compounds.

Formation of chelate complexes

As mentioned before, we used MEA as a representative chelating agent to prove the concept of the chelate complex assisted densification. The chelation reaction between MEA and amorphous Cu–In–Se nanoparticles was indirectly verified by investigating the color change of the liquid part of the slurry. This is because the direct observation of the chelate complex formation at the particle surfaces is very difficult. Usually, the occurrence of a chelate reaction is evidenced by color changes in the solution when a true solution precursor is used. In our case, however, the main concern is the chelation at the particle surface, and the corresponding color change must be screened by the dark and opaque particles. In this regard, we investigated the color change of the liquid part of the slurry instead of the particles themselves under the following assumption: if the reaction between MEA and the particles really occurs some of the chelate complexes should be extracted to the liquid part of the slurry and would change the color of that liquid. In other words, the color change of the liquid part of the slurry definitely reflects the occurrence of the chelation reaction at the particle surfaces.

In this concept, to see the color change more clearly, the colloid was centrifuged and the liquid part was separated for investigation. These procedures are illustrated in Fig. 2.

First, as a reference, the liquid part of the original colloid was taken and it was compared with that of the MEA added colloid (Fig. 2). While the extracted liquid of the original colloid (mainly methanol) is colorless and transparent, that of the MEA added colloid is found to be blue colored, confirming the chelate reaction between MEA and nanoparticles.
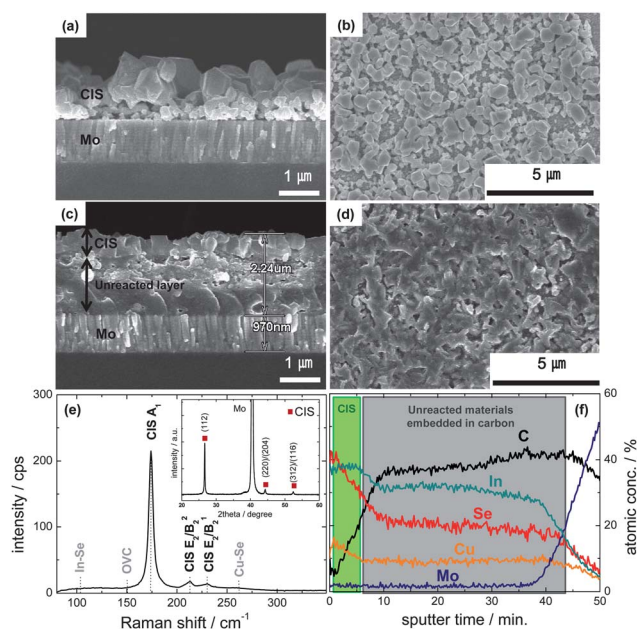
Selenized CIS thin film

The precursor film prepared from the MEA added colloid was selenized with Se vapor. For a comparison, another precursor film prepared from the original colloid without MEA was selenized in the same batch.

Morphologies, crystalline structure and compositional depth profile of the selenized films are presented in Fig. 3. Fig. 3(a) and (b) are the cross-sectional and plane view of the selenized film without MEA addition, respectively. Fig. 3(c) and (d) are SEM images of the film with MEA addition, and its Raman spectrum (with XRD pattern in inset) and AES profile are presented in Fig. 3(e) and (f), respectively.

When the surfaces of precursor particles are not modified by MEA (Fig. 3(a) and (b)), the final selenized film showed a very rough and irregular shaped morphology, which is consistent with our previous report.[18] In this case, growth of the particles up to a few μm range is clearly visible presumably by Ostwald ripening, in which larger particles grew by continuously drawing and consuming materials from smaller ones. However, this left very large voids in the final film, which is opposite to our intention of performing selenization. The irregular growth of the particles resulted in an exposal of bare Mo as shown in Fig. 3(b), leading to a complete short circuiting of the corresponding device. It means that there was not enough viscous flow of precursor materials to fill the voids during selenization, even though the original particles were in amorphous state.

The film formed *via* an MEA assisted route, however, showed a significantly different morphology (Fig. 3(c) and (d)). Firstly, it had a double-layered structure with a 500 nm thick crystalline top layer and a 2 μm thick amorphous-like bottom layer. From

Fig. 2 Confirmation of the formation of chelate complexes by the reaction between MEA and Cu–In–Se nanoparticles.

Fig. 3 (a) Cross-sectional and (b) plane views of the CIS film fabricated by selenization of the precursor film prepared from the Cu–In–Se nanoparticle/methanol colloid without MEA addition. (c) Cross-sectional and (d) plane views of the film fabricated from MEA added colloid. (e) Raman spectra and XRD pattern (inset) and (f) AES depth profile of the film shown in (c) and (d).

the Raman spectrum (Fig. 3(e)), XRD pattern (inset in Fig. 3(e)) and AES depth profile of the same sample (Fig. 3(f)), it was found that the top layer is a chalcopyrite CIS with a strong (112) preferred orientation without any binary phases of Cu–Se and In–Se. AES data further revealed that the bottom layer contains a significant amount of carbon (up to 40 at%) as well as Cu, In and Se elements, implying that unreacted precursor materials are embedded in carbon residue even after the high temperature selenization. This is probably due to unoptimized pre-treatment, and further processing refinement such as a longer drying process at higher temperature will likely lead to a carbon-free precursor film.

Regarding the morphology of the top CIS layer in terms of its roughness and density, it is clear that MEA addition is beneficial in that the film shown in Fig. 3(c) and (d) has a much flatter surface, larger grains and a higher surface coverage (lower porosity) with enhanced lateral connections between grains than that shown in Fig. 3(a) and (b) has. We attribute this improvement in film morphologies to the lower activity of the precursor particles modified with MEA chelate complexes. This should allow for film densification due to more enhanced structural relaxation and viscous flow by delaying the crystallization of the film to higher temperatures.

Apart from the morphological improvement of the film, Fig. 3(f) reveals that the selenized film is significantly deficient in Cu and Se. Apparently, the top layer has a composition similar to the ordered vacancy compound (OVC) with Cu : In : Se = 1 : 3 : 5, but from the fact that this film has no OVC phase (Raman spectrum, Fig. 3(e)) it should be considered as a mixture of α-CIS and extra In-compounds with very low crystallinity.

Considering that the as-synthesized particles had atomic ratios close to Cu : In : Se = 0.9 : 1 : 2, the Cu and Se loss is thought to be related to the complex formation of these elements. From the fact that our nanoparticles are mainly composed of Cu–Se and In–Se binaries, one possible scenario is that if the dissociation of Cu–MEA complexes during the high temperature process is easier than In–MEA complexes, then some of the Cu–Se binaries at the surface region has a possibility to evaporate in the form of Cu–Se gases before constructing CIS because there may be a significant unbalance between the numbers of Cu–Se and In–Se binaries, i.e., large amount of Cu–Se phases but much less amount of (reactive) In–Se phases. This hypothesis is partly supported by the previous paper reporting that Cu_2Se can be easily evaporated at around 600 °C.[22] The high surface energy of our nano-sized Cu–Se particles might enhance their evaporation and/or lower the evaporation temperature.

Device performances

We fabricated solar cells using the CIS films prepared from the MEA added colloid, and the device showed a remarkable conversion efficiency of 4.41% with a V_{OC} of 0.35 V, a J_{SC} of 28.4 mA cm^{-2} and an FF of 0.44 (Fig. 4(a)), in spite of the compositional imperfections of the top CIS layer and the presence of the thick unreacted bottom layer. Considering that the device fabricated with the rough and irregular shaped CIS film shown in Fig. 3(a) and (b) was completely short circuited by a direct contact between CdS/ZnO and Mo layers through the large voids, this efficiency increase is believed to have originated

from improvement in the density of the CIS top layer. Especially, the higher surface coverage and lower porosity of the CIS film obtained by the MEA addition definitely lead to the lower probability of short-circuiting.

External quantum efficiency (EQE) data (Fig. 4(b)) exhibited a long end tail with a gradually decreasing EQE from about 570 nm, which is attributed to a short minority carrier lifetime and/or incomplete light absorption. The J_{SC} value calculated
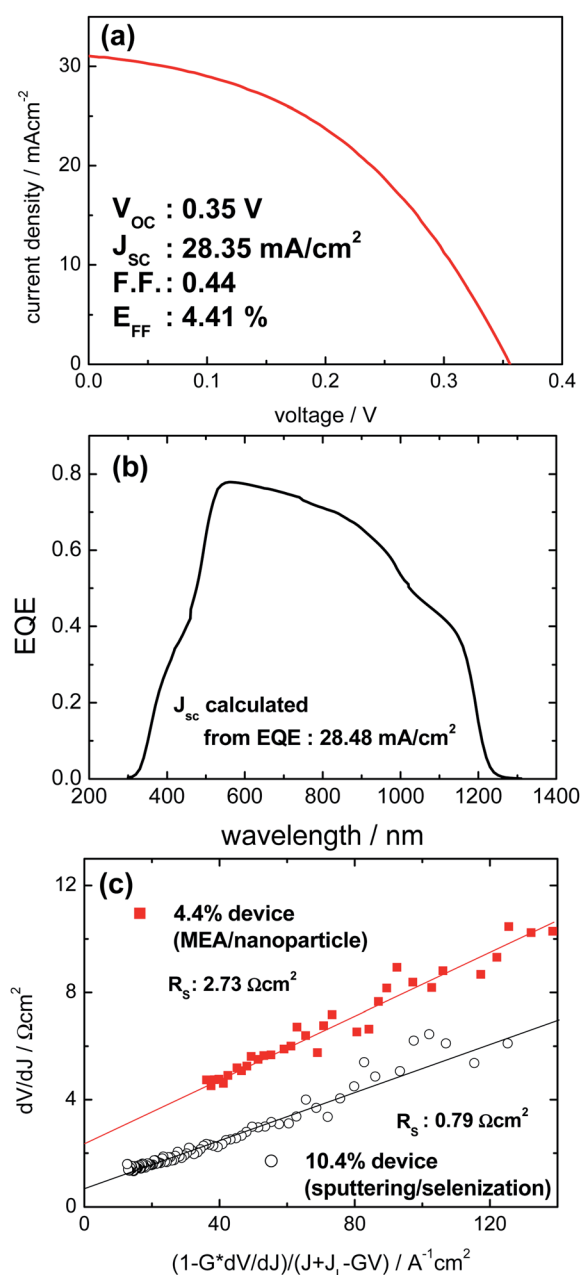
Fig. 4 (a) The illuminated I–V curve of the solar cell fabricated from the MEA added colloid, measured under AM 1.5G, 100 mW cm^{-2} and 25 °C conditions. (b) The EQE curve of the same device. (c) The R–J curve redrawn from (a). For a comparison, in (c), the R–J curve of a CIS solar cell with conversion efficiency of 10.44% prepared by a sputtering/selenization process is presented together.

from the EQE data was 28.48 mA cm^{-2}, which is very similar to that measured from the solar simulator (Fig. 4(a)).

Fig. 4(a) was further converted to dJ/dV vs. V and R–J forms to extract shunt conductance (G) and series resistance (R_S), respectively. From the dJ/dV vs. V relation (not shown here), G was measured to be 14.1 mS cm^{-2}. This value is high compared to typical G values of high efficiency CIGS solar cells (<1 mS cm^{-2}), which is attributed mainly to a still imperfect surface coverage, as shown in Fig. 3(d), and partly to the excessive Cu deficiency of our CIS film.

For the R–J curve (Fig. 4(c)), for a comparison, another R–J curve of a CIS device with conversion efficiency over 10% fabricated by the sputtering/selenization technique in our laboratory is shown together. Fig. 4(c) demonstrates that the nanoparticle based device suffers from much higher R_S compared to the 10.44% CIS device presumably due to the thick unreacted layer.

In spite of the still low conversion efficiency, the strategy of forming chelate complexes at the surface of amorphous nanoparticles is shown to be very effective to obtain absorber films with higher density. In particular, it is expected to provide us a very economical way to form CIS films by making it possible to fully utilize the advantages of the low temperature colloidal particle preparation route, i.e., very short reaction time (~1 minute) and no need of external heating. Finer tuning of composition such as increasing Cu and Se contents in the top layer, reducing the carbon contents in the bottom layer and increasing the absorber layer thickness will likely further improve the device performance.

Conclusion

A novel and simple process for fabrication of a CIS absorber layer using amorphous Cu–In–Se nanoparticles as precursor materials and a chelating agent (MEA) is reported. The main intention of using a chelating agent is to enhance the viscous flow of precursor materials during selenization by lowering their activity due to the formation of chelate complexes at particle surfaces and hence delaying the onset of crystallization to a higher temperature. The CIS films formed by selenization of the precursor films with chelate complexes showed remarkably improved morphology in terms of reduction in roughness and porosity compared to those prepared without using a chelate agent. Based on this approach, a cell efficiency of up to 4.41% was demonstrated for the device fabricated from MEA-added colloid, while that fabricated from MEA-free particles showed a complete short circuiting behavior. Consequently, the strategy of forming chelate complexes at the surface of amorphous nanoparticles is shown to be very effective to obtain absorber films with higher density. It further provides us a very economical way to form CIS films by making it possible to fully utilize the advantages of the low temperature colloidal particle preparation

route, i.e., very short reaction time (~1 minute) and no need of external heating.

References

1 I. Repins, M. A. Contreras, B. Egaas, C. DeHart, J. Scharf, C. L. Perkins, B. To and R. Noufi, *Progr. Photovolt.: Res. Appl.*, 2008, **16**, 235.
2 M. A. Green, K. Emery, Y. Hishikawa and W. Warta, *Prog. Photovolt.: Res. Appl.*, 2011, **19**, 84.
3 C. Eberspacher, C. Fredric, K. Pauls and J. Serra, *Thin Solid Films*, 2001, **387**, 18–22.
4 C. J. Hibberd, E. Chassaing, W. Liu, D. B. Mitzi, D. Lincot and A. N. Tiwari, *Prog. Photovolt.: Res. Appl.*, 2009, **18**, 434.
5 D. W. Benjamin, T. C. Stephen and C. Yi, *J. Am. Chem. Soc.*, 2010, **132**, 6642.
6 S. J. Ahn, K. H. Kim, J. H. Yun and K. H. Yoon, *J. Appl. Phys.*, 2009, **105**, 113533-1–113533-7.
7 D. L. Schulz, C. J. Curtis, R. A. Flitton, H. Weisner, J. Keane, R. J. Matson, K. M. Jones, P. A. Parilla, R. Noufi and D. S. Ginley, *J. Electron. Mater.*, 1998, **27**, 433.
8 S. J. Ahn, C. W. Kim, J. H. Yun, J. C. Lee and K. H. Yoon, *Sol. Energy Mater. Sol. Cells*, 2007, **91**, 1836.
9 Y. G. Chun, K. H. Kim and K. H. Yoon, *Thin Solid Films*, 2005, **480–481**, 46.
10 C. Yu, J. C. Yu, H. Wen and C. Zhang, *Mater. Lett.*, 2009, **63**, 1984.
11 Y. Jiang, Y. Wu, X. Mo, W. C. Yu, Y. Xie and Y. T. Qian, *Inorg. Chem.*, 2000, **39**, 2964.
12 Q. Y. Lu, J. Q. Hu, K. B. Tang, Y. T. Qian, G. E. Zhou and X. M. Liu, *Inorg. Chem.*, 2000, **39**, 1606.
13 J. Tang, S. Hinds, S. O. Kelly and E. H. Sargent, *Chem. Mater.*, 2008, **20**, 6906.
14 M. G. Panthani, V. Akhavan, B. Goodfellow, J. P. Schmidtke, L. Dunn, A. Dodabalapur, P. Barbara and B. A. Korgel, *J. Am. Chem. Soc.*, 2008, **130**, 16770.
15 Q. Guo, S. J. Kim, M. Kar, W. N. Shafarman, R. W. Birkmire, E. A. Stach, R. Agrawal and H. W. Hillhouse, *Nano Lett.*, 2008, **8**, 2982.
16 Q. Guo, G. M. Ford, H. W. Hillhouse and R. Agrawal, *Nano Lett.*, 2009, **9**, 3060.
17 S. J. Ahn, K. H. Kim, Y. G. Chun and K. H. Yoon, *Thin Solid Films*, 2007, **515**, 4036.
18 S. J. Ahn, K. H. Kim, A. Cho, J. Gwak, K. Shin, S. K. Ahn and K. H. Yoon, *ACS Appl. Mater. Interfaces*, 2012, DOI: 10.1021/am201755q.
19 R. W. Schwartz, *Chem. Mater.*, 1997, **9**, 2325.
20 S. Y. Lee and B. O. Park, *Thin Solid Films*, 2008, **516**, 3862.
21 A. Y. Oral, E. Mensur, M. H. Aslan and E. Basaran, *Mater. Chem. Phys.*, 2004, **83**, 140.
22 S. C. Park, S. H. Kwon, J. S. Song and B. T. Ahn, *Sol. Energy Mater. Sol. Cells*, 1988, **50**, 43.